International Journal of Applied Research 2020; 6(6): 370-373

ISSN Print: 2394-7500
ISSN Online: 2394-5869
Impact Factor: 5.2
IJAR 2020; 6(6): 370-373
www.allresearchjournal.com
Received: 19-04-2020
Accepted: 21-05-2020

Dr. Anshu Anand
Department of Physics CCS University Meerut,
Uttar Pradesh, India

Corresponding Author:
Dr. Anshu Anand
Department of Physics CCS University Meerut,
Uttar Pradesh, India

Rheological properties of liquid particle suspensions

Dr. Anshu Anand

Abstract
The observations of Couette flow of liquid-particle suspensions are explained in detail. In the lattice-Boltzmann models, the fluid techniques are combined with those of molecular mechanics for the Newtonian motion of stable colloidal particles. The key justification for this component of the work was to provide benchmarking for future liquid-particle suspension simulations. We explain in the rheological properties of 3D (2D) suspensions the position of particle shape, shear rate, and solid volume fraction (area fraction), i.e. concentration. As a function of shear intensity and emphasis, the viscosity of suspensions is studied.

Keywords: Couette flow, liquid-particle suspensions, shear rate, and solid volume fraction

Introduction

In many industrial processes, suspensions of submicrometer-sized particles occur, for example in the paper industry, in emulsion technology, in environmental processes, and in biological systems. Therefore, the flow dynamics and rheological properties of such liquid-particle suspensions are generally known [1]. Due to their complex microstructure, suspension rheology can rely on several factors such as fraction of particle volume, particle size, particle form, ionisation, liquid suspension, flow rate, and shear rate.

It has also been shown recently that polydispersity can have a major influence on particle suspension hydrodynamics. In addition, attractive and repulsive interactions between the particles have been shown to have a substantial influence on the rheology of the suspension. One can better understand how for example, particle interactions influence the suspension's rheological properties to increase particle concentration, and the suspension's two-phase character can give rise to complicated microstructural activity in different flow regimes [2-5].

For two main factors, the scientific (both empirical and numerical) analysis of suspension rheology is complicated. Second, many length and time scales are involved in the hydrodynamic interactions between the suspended particles. Short-range lubrication forces, which are movements between two bodies, occur. There is an intermediate range in which interactions of many-body hydrodynamics are essential. Long-range relationships still occur that must be 'renormalized' appropriately. Second, in order to calculate the rheology, the exact knowledge of the forces and stresses for a given particle configuration is not adequate since an average is needed over various particle configurations. The product of an interaction between the external driving forces (e.g. an induced shear flow or gravity) and the 'internal' hydrodynamics, i.e. the inter-particle and Brownian forces, is these arrangements themselves. Therefore, the system is fully coupled [6]. Extremely idealised structures, such as dilute spherical suspensions at low shear speeds, have typically been believed by theoretical methods for these reasons. Experimental awareness is often limited since even the most widely used viscometer operation is not always well managed. Traditionally, theoretical and computational experiments have been focused on diverse spectrum models. These models, however often contain many microscopic origin parameters that are difficult to determine. Simulation outcomes for particulate suspensions can also be more beneficial and have instant and broad applicability. Detailed studies of microstructures have indeed been possible on the theoretical side by direct simulation of the motions of individual particles. Such tests, however, are still computationally intensive, and typically require approximations.

Liquid-particle suspension viscosity

Several dimensionless parameters can depend on the viscosity of the suspension of monodisperse spheres. The most important of these are the solid volume fraction ϕ = (4/3)πρn R and the Peclet number Pe = γ d 2 /D. Here d is the particle diameter, ρn the particle number density, R the radius of the particles, γ w the shear rate, and D0 the diffusion coefficient related to the Brownian motion of the particles. The hydrodynamic shear forces ratio and the diffusive Brownian forces acting on the suspended particles are represented by the Peclet number. The Brownian forces appear to bring the suspended particles back to their configuration of equilibrium, which is constantly disrupted by the particle-acting hydrodynamic shear forces. If the Brownian powers (as is the case here are omitted, the number of Shear Reynolds.

Reγ = ρ d 2u (μ H) = γ d 2 ν is used to characterise the flow conditions instead of the Peclet number. Here ν f is the kinematic viscosity of the carrier fluid, and ρ f is its density. For 2D discs, e.g., the area fraction is $\phi = \pi\rho R^2$

Studies Benchmark for the Lb Process

To ensure the correctness and precision of our outcomes and our simulation codes, we carried out various benchmark tests. As shown earlier by the LB approach for fluid-flow simulations, strong alignment was found between the theoretical and simulated velocity profiles in a channel flow.

An simple measure for suspension simulations is also to equate particles' hydrodynamic radius R_H with their nominal radius R. By simulating fluid flow through an infinite array of discs in 2D or spheres in 3D, the hydrodynamic radius R_H was derived. The simulation was performed by placing a solid fixed particle in an arbitrary location in a periodic cubic box with side length L and subject to fluid stream with velocity U. Analytical expressions for the drag coefficient are known for both 2D and 3D systems [7, 8] and the latter is given by

$$F_D = 6\pi\mu_f R_H U \Big/ \left[\frac{1}{R_H} - \frac{2.837}{L} + \frac{4.19}{L^3} R_H^2 - \frac{27.4}{L^6} R_H^5\right]$$

In addition, in the centre of a pipe, strong agreement was found for a disc-like particle moving under an external force, such as gravity, in the forces induced on the particle and the walls, between our results and those measured by FEM or the LB method. The hydrodynamic forces on a fixed disc with forced counter clock wise rotation near a moving wall were simulated and compared with the effects of a commercial finite-volume solver (Fluent) in another benchmark analysis. Many particle radii and two separate distances between the middle of the particle and the moving wall have been simulated.

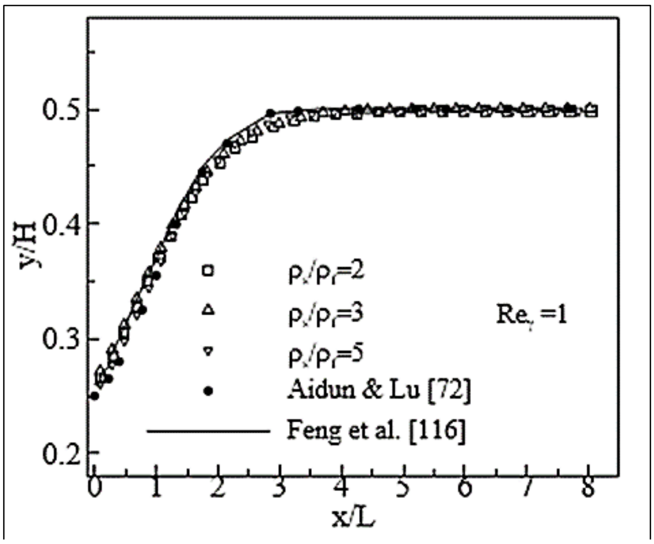

Fig 1: Comparison of the lateral migration of a particle in a vertical channel of length L (x direction) and width H (y direction) with the results of Aidun and Lu [9], and Feng *et al.* [10], for Reγ = 1.

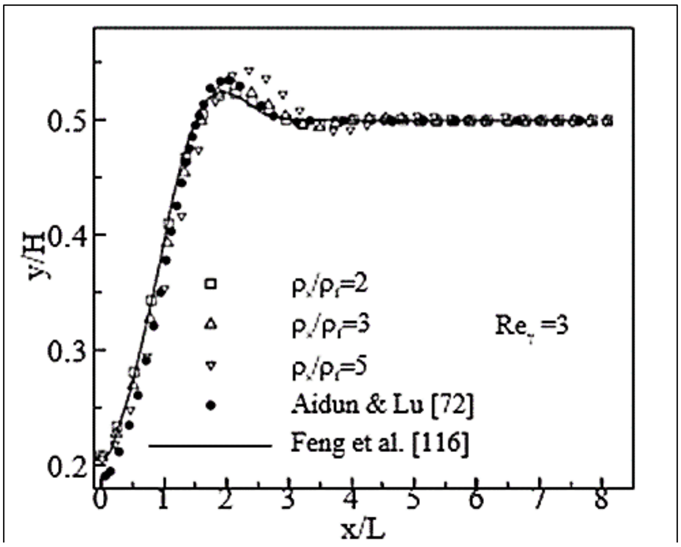

Fig 2: Comparison of the lateral migration of a particle in a vertical channel with the results of Aidun and Lu [9], and Feng *et al.* [10], for Reγ = 3.

As a particle initially positioned near a wall migrated to the centre of the pipe, as seen in Figures 1 and 2, with three different ratios of partial density to fluid density, we found strong agreement with their findings.

Viscosity in Suspensions in Liquid-Particle

The suspension was positioned between two moving solid walls aligned in the x direction and separated by a distance H, to mimic the Couette flow of a liquid-particle suspension. The walls moved with speed uw in opposite directions. Couette-flow conditions are thus created with the mean shear rate γ w = 2uw H. It is evident that the viscosity in the case of star-shaped particles (a cross-shaped combination of two perpendicular ellipsoidal particles, with two different axis ratios a and major axes l: a = 4.3, l = 17.2 and a = 2.7, l = 8.0) increases much more rapidly with increasing solid volume fraction than in the case of disc-shaped particles. Instead, the viscosity of ellipsoidal particles quite closely follows that of disc-like particles (not shown).

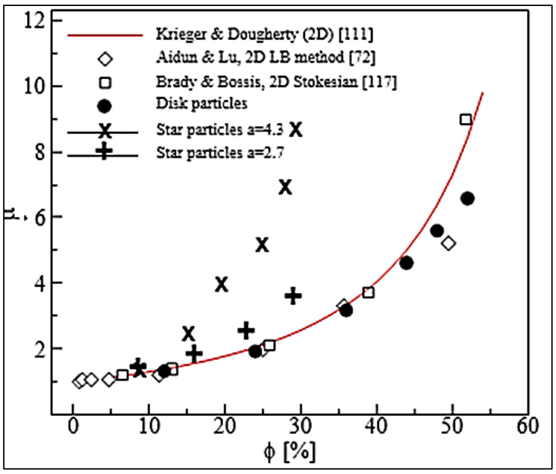

Fig 3: The simulated relative apparent viscosity μr for disk–shaped and star-shaped particles as a function of the solid volume fraction ϕ for Reγ ≈ 1.0.

A simplified version of the 3D simulation of Couette flow of monodispersed spherical particles was also carried out such that the particles were restricted to move only in one layer along the xy plane. In these monolayer simulations the shear Reynolds number was varied between 0.1 and 15, and ϕ between 6% and 52%.

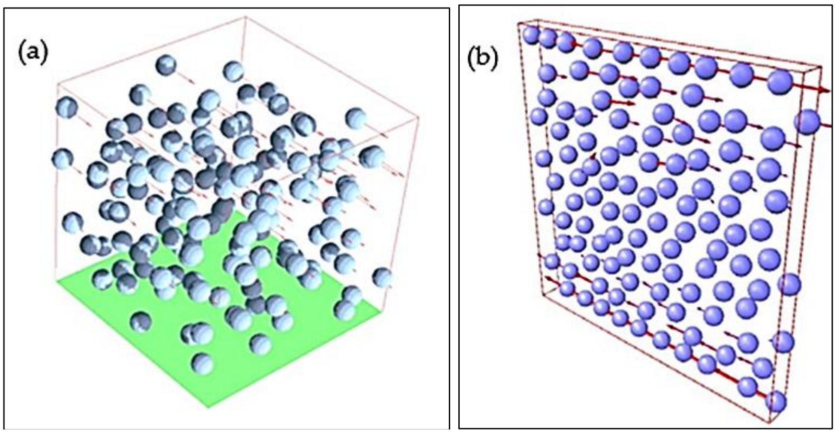

Fig 4: (a) A snapshot of a shear flow of suspended spherical particles as simulated by the three-dimensional LB method. (b) A snapshot of a shear flow of a monolayer of suspended spherical particles as simulated by the 3D(m) LB method.

We computed the relative apparent viscosity μr of the suspension for both versions of the 3D simulations

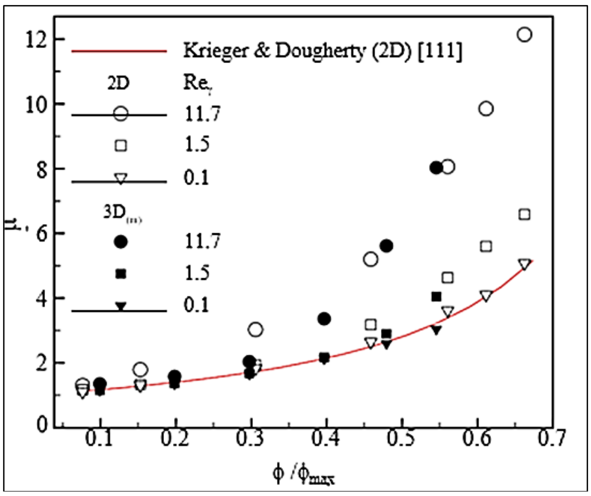

Fig 5: The simulated relative apparent viscosity μr for disk–like (2D) and spherical 3D(m) particles restricted to move in a monolayer as a function of normalised solid volume fraction ϕ / ϕmax : ϕmax = 0.785 in 2D and 0.605 in 3D. Results are shown for three values of Reγ. Also shown is the 2D version of Krieger formula.

As seen in Figure 5, the magnitude of relative apparent viscosity for the corresponding scaled concentration values is observed to be greater in the 2D framework than in a 3D monolayer of spheres. The divergence from the Krieger formula takes place at a lower concentration to increase the shear rate, which is required due to shear thickening. Note that the results for dilute 3D(m) systems follow closely the Krieger formula, even for relatively high Reynolds numbers. For increasing solid volume fraction, the 3D relative viscosity seems to approach the corresponding 2D value.

Conclusion

We have performed many other benchmark experiments, such as the propagation of stress around a shear flow particle and the different relative motion of particles near a wall. In addition, recorded benchmark tests demonstrate that the approach implemented here is sufficient for practical simulations of suspension. Based on the above measurements and benchmarks, we should infer that the fundamental physical context of the model used here is correct.

References

1. Barnes HA *Dispersion rheology:* 1980 (Royal Soc. of Chem., London) 1981.
2. Thies-Weesie DME, Philipse AP, Lekkerkerker HNW, J Colloid Interface Sci 1996;177:427.
3. Chang C, Powell RL, Fluid J Mech 1993;253:1.
4. Wagner NJ, Woutersen ATJM, Fluid Mech J. 1994;278:268.
5. Russel WB, Saville DA, Schowalter WR. Colloidal dispersions (Cambridge University Press) 1992.
6. Happel J, Brenner H. Low-Reynolds Number Hydrodynamics (Kluwer, Dordrecht) 1991.
7. Jackson GW, James DF, Canadian J. Chem. Engrg 1986;64:370.
8. Hashimoto H, Fluid Mech J. 1959;5:317.
9. Aidun CK, Lu Y, Stat J. Phys 1995;81:49.
10. Feng J, Hu HH, Joseph DD, Fluid Mech J. 1994;261:95.
11. Krieger IM, Dougherty TJ, Tran. Soc. Rheol 1959;3:137.
12. IM Krieger, Adv. Colloid Interface Sci 1972;3:111.